



ISSN: 2447-3359

REVISTA DE GEOCIÊNCIAS DO NORDESTE

*Northeast Geosciences Journal*

v. 10, nº 1 (2024)

<https://doi.org/10.21680/2447-3359.2024v10n1ID34612>



## Estimativa da turbidez da água utilizando imagens de RPA's associadas às técnicas de Machine Learning

### *Water turbidity estimation using RPA's images and Machine Learning techniques*

Laura Coelho de Andrade<sup>1</sup>; Tiago Oliveira Lopes<sup>2</sup>; Nilcilene das Graças Medeiros<sup>3</sup>; Italo Oliveira Ferreira<sup>4</sup>; Afonso de Paula dos Santos<sup>5</sup>; William Rodrigo Dal Poz<sup>6</sup>

- <sup>1</sup> Federal University of Viçosa/Department of Civil Engineering, Viçosa/MG, Brazil. Email: laura.andrade@ufv.br  
**ORCID:** <https://orcid.org/0000-0003-3693-2208>
- <sup>2</sup> Federal University of Viçosa/Department of Civil Engineering, Viçosa/MG, Brazil. Email: tiago.lopes@ufv.br  
**ORCID:** <https://orcid.org/0009-0007-0067-6923>
- <sup>3</sup> Federal University of Viçosa/Department of Civil Engineering, Viçosa/MG, Brazil. Email: nilcilene.medeiros@ufv.br  
**ORCID:** <https://orcid.org/0000-0003-0839-3729>
- <sup>4</sup> Federal University of Viçosa/Department of Civil Engineering, Viçosa/MG, Brazil. Email: italo.ferreira@ufv.br  
**ORCID:** <https://orcid.org/0000-0002-4243-8225>
- <sup>5</sup> Federal University of Viçosa/Department of Civil Engineering, Viçosa/MG, Brazil. Email: afonso.santos@ufv.br  
**ORCID:** <https://orcid.org/0000-0001-7248-4524>
- <sup>6</sup> Federal University of Viçosa/Department of Civil Engineering, Viçosa/MG, Brazil. Email: dalpoz@gmail.com  
**ORCID:** <https://orcid.org/0000-0001-9532-3643>

**Abstract:** The water quality in reservoirs is crucial for the preservation of ecosystems and human health. Turbidity, which assesses the presence of suspended particles, is an important indicator typically measured on-site with expensive equipment. However, with the advancement of Artificial Intelligence (AI), it is possible to estimate turbidity using orbital images associated with indices such as NDTI (Normalized Difference Turbidity Index). In addition to orbital sensors, another technology widely used for various purposes is remotely piloted aircraft (RPA), which enables the generation of digital photogrammetric products like Digital Elevation Models and high-detail Orthophotos. In this context, this study aims to estimate turbidity in reservoirs using RPA images and Machine Learning techniques such as Artificial Neural Networks (ANN), Support Vector Machine (SVM), Gradient Boosting Machine (GBM), and Random Forest (RF). To achieve this, on-site surveys were conducted using turbidimeters and RPAs to obtain data for regression analysis to correlate the information. Based on the results obtained, it was observed that the prediction of turbidity using RF and ANN exhibited the best performance.

**Keywords:** Remote Sensing; Water quality; Data Analysis; Artificial Intelligence.

**Resumo:** A qualidade da água em reservatórios é fundamental para a preservação dos ecossistemas e da saúde humana. A turbidez, que avalia a presença de partículas suspensas, é um indicador importante, geralmente medido in loco com equipamentos onerosos. No entanto, com o avanço da Inteligência Artificial (IA), é possível estimar a turbidez usando imagens orbitais associadas a índices como o NDTI (Normalized Difference Turbidity Index). Além de sensores orbitais, outra tecnologia que vem sendo muito utilizada para vários fins são as aeronaves remotamente pilotadas (RPA's) que possibilitam a geração de produtos fotogramétricos digitais como Modelos Digitais de Elevação e Ortofotografias em grandes níveis de detalhes. Nesse sentido, este estudo visa estimar a turbidez em reservatórios usando imagens de RPA e técnicas de Machine Learning como a RNA (Redes Neurais Artificiais), SVM (Support Vector Machine), GBM (Gradient Boosting Machine) e RF (Random Forest). Assim, foram feitos levantamentos in loco com o equipamento turbidímetro e com RPA para obtenção dos dados para análise de regressão para correlacionar os dados. Por meio dos resultados obtidos, pôde-se perceber que a predição da turbidez utilizando o RF e a RNA apresentaram os melhores desempenhos.

**Palavras-chave:** Sensoriamento Remoto; Qualidade da água; Análise de dados; Inteligência Artificial.

## 1. Introduction

Reservoirs and water bodies play a fundamental role in ensuring water supply for the population. They store large quantities of this resource, which is used in various activities such as human consumption, agriculture, and hydroelectric power generation (Gleick, 2003; Awange, 2022). Continuous monitoring of these water bodies is essential to identify potential problems such as water volume reduction or pollution, allowing corrective measures to be taken before more serious issues arise (O'Reilly *et al.*, 2003; Woolway *et al.*, 2020). Depth measurement of reservoirs is one of the main forms of monitoring, enabling the assessment of stored water quantity and the identification of sedimentation or erosion in the water body (Ferreira, Rodrigues, Santos, 2015; Andrade *et al.*, 2020).

Moreover, turbidity is also an important factor that can affect water quality. According to Hossain, Mathias, and Blanton (2021), turbidity is defined as a measure of water transparency derived from light scattering due to the presence of suspended particulate materials in a water body. According to Xiao *et al.* (2021), evaluating variations in turbidity is an essential tool for understanding how sediments or suspended particles are distributed in the aquatic environment, and it provides practical information for studying how pollutants settle, decompose, and diffuse in the water.

According to Allam, Khan, and Meng (2020), remote sensing is an efficient technique for monitoring the aquatic environment as it allows real-time and large-scale assessment of different aspects. Through various platforms such as artificial satellites and RPAs (Remotely Piloted Aircrafts), detailed images and information about the aquatic environment can be obtained, enabling a more accurate assessment of relevant environmental variables such as water quality, the presence of pollutants, turbidity, among others.

According to Prior *et al.* (2020), RPAs offer users flexibility in obtaining information, allowing precise control over the spatial resolution of captured images. With this technology, data can be collected in dangerous or hard-to-access areas, and the spatial resolution of the image to be acquired can be planned in advance. Additionally, it can be remotely controlled, ensuring user safety and making data collection more efficient.

Technological advancements have also led to the optimization of Artificial Intelligence and consequently, Machine Learning techniques. The development of these tools associated with optical remote sensing, especially in environmental studies, can provide significant advances and conveniences in information gathering. Authors such as Li *et al.* (2023) used Sentinel-3 OLCI images to estimate water turbidity in a Chinese lake, employing algorithms like SR (Simple Regression), PLSR (Partial Least Squares Regression), SVR (Support Vector Regression), BP (Backpropagation neural network), KNN (K-nearest neighbor), RF (Random Forest), and XGBoost (Extreme Gradient Boosting). In this study, RF showed superior performance over the others, achieving an  $R^2$  of 0.92 and an RMSE of 12.65 NTU (Nephelometric Turbidity Unit). Ma *et al.* (2021) conducted studies on water turbidity estimation using Sentinel 2A images and machine learning algorithms, finding GBDT (Gradient Boosting Decision Tree) as the best regression method, presenting better performance values.

In this context, the main objective of this work is to estimate the turbidity of water bodies using Machine Learning algorithms: SVM (Support Vector Machine), GBM (Gradient Boosting Machine), RF (Random Forest), and ANN (Artificial Neural Networks) and RPA images.

## 2. Study Area

The study area is located in the city of Viçosa, MG, within the Federal University of Viçosa, and covers approximately 1.16 hectares (Figure 1).

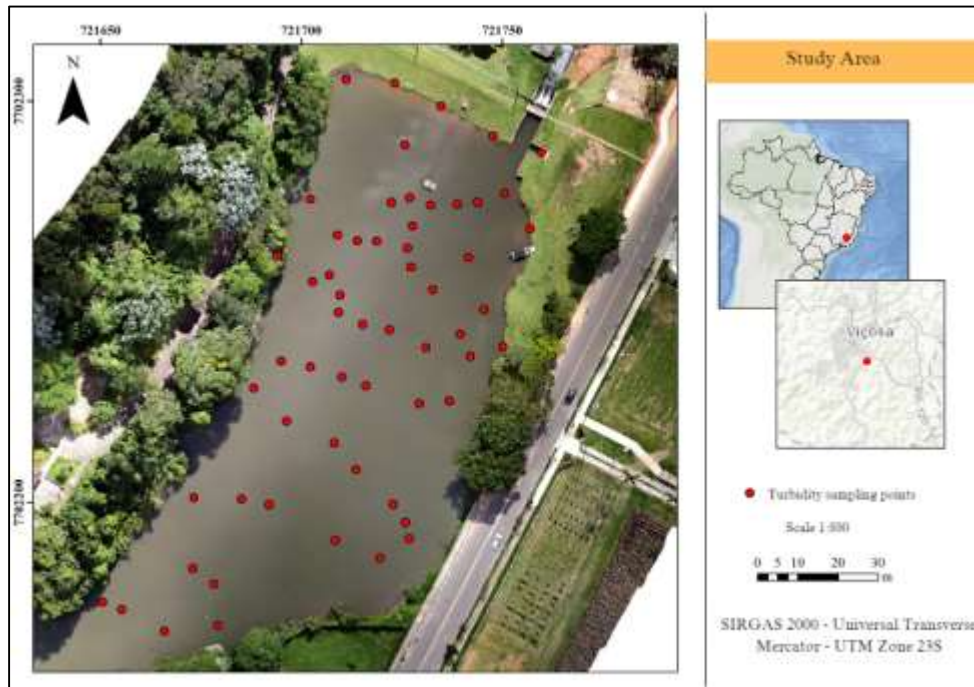


Figure 1 – Study area showing the water turbidity sampling points.  
Source: Authors (2023).

It is important to highlight that this water body, like other reservoirs present at the University, plays a crucial role in supplying the population of Viçosa during the dry season.

### 3. Methodology

The methodology adopted in this study can be observed in the flowchart presented in Figure 2.

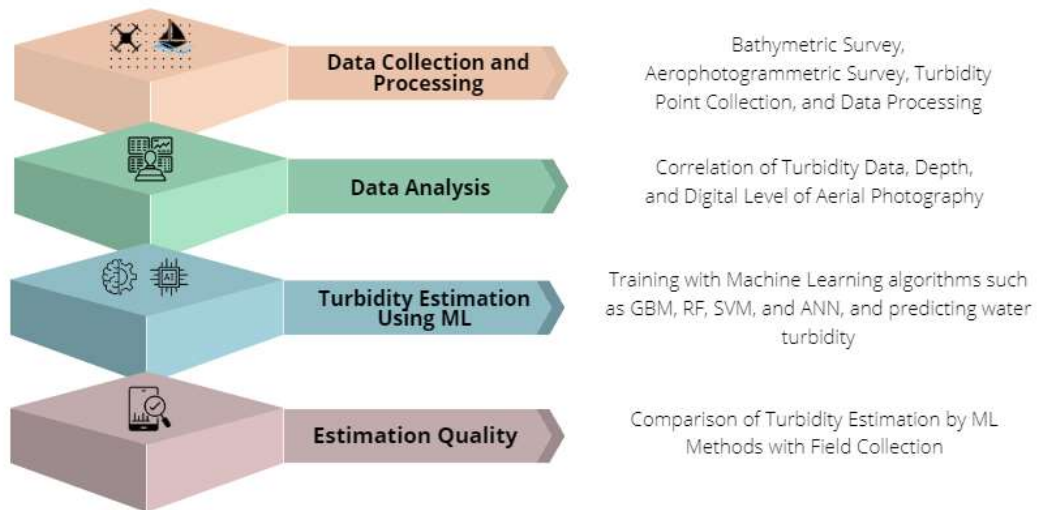


Figure 2 – Methodology flowchart.  
Source: Authors (2023).

### 3.1. Data Collection and Processing

To initiate the study, an aerophotogrammetric survey was necessary. A flight plan was executed with 80% longitudinal overlap and 70% lateral overlap at an altitude of 80 meters. The flight was conducted using a Mavic Air 2S aircraft, and 55 photographs were acquired with an average GSD of 2.66 cm/pixel. Additionally, 7 control points and 7 check points were collected using the GNSS (Global Navigation Satellite System) RTK (Real-Time Kinematic) from Topomap, model T10.

The aerophotogrammetric data processing was performed using Agisoft Metashape software (AGISOFT LCC, 2023), where the images were imported and aligned. Subsequently, the control points were imported, and the dense point cloud was generated, modeled, and textured, creating the Digital Surface Model (DSM). Finally, the orthomosaic of the photographs was generated using the DSM and the camera calibration information.

In addition, water turbidity points were collected using the TU430 turbidimeter from AKSO (Figure 3), and the GNSS RTK T10 from Topomap was used for georeferencing the samples (Figure 4). The points were collected randomly with a density of approximately 51 samples/ha. Authors like Zhao *et al.* (2011), Bonansea *et al.* (2015), and Su and Chou (2015) collected samples from water bodies and concluded that at least 9 samples/ha are necessary for a correct understanding of water turbidity variability in the study area. The distribution of samples is shown in Figure 1. Statistical analyses were performed on the turbidity samples for verification.



*Figure 3 – Digital Turbidimeter TU340.  
Source: AKSO (2023).*



*Figura 4 – GNSS RTK T10.  
Source: Topomap (2023).*

The bathymetric survey was also conducted to complement the analysis, using a single-beam echo sounder E20 from Teledyne Odom, operating at a frequency of 210 kHz. For the horizontal positioning of the boat, a pair of GNSS RTK receivers was employed. Six longitudinal survey lines and two transverse verification lines were surveyed. These bathymetric data were processed using Hypack 2021 software (HYPACK, 2021) and interpolated using the IDW (Inverse Distance Weighted) method in ArcGis 10.5 software (ESRI, 2016) to generate the Digital Depth Model (DDM), where depth values are displayed continuously.

### 3.2. Data Analysis

After creating the orthomosaic, it was possible to correlate the digital pixel values with the bathymetry DDM and water turbidity samples. To better match the data, the turbidity samples were also interpolated using the IDW interpolator, thus creating a Digital Turbidity Model (DTM), as done by Dezordi *et al.* (2019).

Additionally, the NDTI (Normalized Difference Turbidity Index) was calculated to be used later to improve the training of Machine Learning algorithms (Equation 1).

Equation 1 Normalized Difference Turbidity Index (NDTI)

$$NDTI = \frac{\rho_{red} - \rho_{green}}{\rho_{red} + \rho_{green}} \quad (1)$$

Where  $\rho_{red}$  are the brightness values of the orthophoto for the red light band, and  $\rho_{green}$  are the brightness values for the green light band.

NDTI is an index created by Lacaux *et al.* (2007) and used by authors such as Cahalane *et al.* (2019) for depth prediction with Landsat 8, Pleiades, and RapidEye images. These authors observed that water turbidity can result in higher radiance values for the visible and NIR (Near Infra-Red) bands, underestimating depths in deeper locations (6m to 10m) (CASAL *et al.*, 2019). Lacaux *et al.* (2007) also state that in turbid water locations, the electromagnetic radiation corresponding to red light can have a higher response compared to green light.

### 3.3. Turbidity Estimation Using Machine Learning

Using the points generated from the DTM (Digital Turbidity Model) with the correlated values of the orthophoto bands, depth, and the aforementioned NDTI, a database was created, also containing the UTM coordinates of the points for insertion into the RF (Random Forest), GBM (Gradient Boosting Machine), SVM (Support Vector Machine), and ANN (Artificial Neural Networks) algorithms in R software (R CORE TEAM, 2023).

For all algorithms, 70% of the sample points were randomly selected for training the empirical methods to be evaluated, and the remaining 30% for prediction testing. Authors like Verrelst *et al.* (2012), Cahalane *et al.* (2019), and Mateo-Pérez *et al.* (2020) used this data separation method for training and testing, achieving unbiased results with good performance.

Additionally, to ensure consistent evaluation of the algorithms, a "seed" was defined so that the algorithms would always select the samples in the same order, i.e., always using the same data set.

For SVM, the "svmRadial" training method was used as it provided the best results for the selected sample. Authors like Hong *et al.* (2016) and Harimoorthy and Thangavelu (2021) also employed this method for better predictions.

For GBM and RF algorithms, the "gbm" and "rf" methods were used, respectively, as it is the standard for making predictions with these Machine Learning methods. The ANN had one hidden layer, four intermediate layers corresponding to the brightness values for the visible bands of the orthophoto, as well as the calculated NDTI values, and one output layer corresponding to turbidity. Additionally, the ANN was trained and evaluated using the "neuralnet" package, which employs the "backpropagation" tool in the learning process.

### 3.4. Quality Estimation

To evaluate the obtained results, an exploratory analysis of the discrepancies found between the reference turbidity values and the values estimated by the aforementioned algorithms was initially conducted.

For subsequent analysis and comparison of all methods, the discrepancies' values addressed in this work were stored using RMSE (Root Mean Square Error), MAE (Mean Average Error), and  $R^2$  (correlation coefficient) (Equations 2, 3, and 4).

Equação 2 Mean Absolute Error (MAE)

$$MAE = \frac{1}{n} \sum_{j=1}^n |t_i - tpredi| \quad (2)$$

Equação 3 Root Mean Square Error (RMSE)

$$RMSE = \sqrt{\frac{1}{n} \sum_{j=1}^n (t_i - tpredi)^2} \tag{3}$$

Equação 4 Correlation Coefficient (R<sup>2</sup>)

$$R^2 = \frac{\sum_{i=1}^n (tpredi - tmedia)^2}{\sum_{i=1}^n (t_i - tmedia)^2} \tag{4}$$

Where *t<sub>i</sub>* corresponds to the observed sample values (collected with the turbidimeter); *tpredi*, is the predicted sample value (obtained by the ML methods); *tmedia*, is the mean of the observed values, and *n* is the number of samples.

The RMSE and MAE are indicators of the precision of the predicted value. Thus, when the estimated turbidity and the predicted turbidity have close values, these indicators approach zero, meaning that the smaller the RMSE and MAE values, the greater the precision found by the method (Yang *et al.*, 2020).

Additionally, to spatialize and better visualize the data, digital turbidity models were generated with the methods used in ArcGIS 10.5 software (ESRI, 2016).

#### 4. Results and Discussion

The first step in implementing the adopted methodology was to perform a statistical analysis of the turbidity data collected in situ using the turbidimeter (Table 1).

*Table 1 – Statistical Analysis of Turbidity Points.*

	Mean	Standard Error	Standard Deviation	Sample Variance	Kurtosis	Skewness	Minimum	Maximum
<b>Turbidity (NTU)</b>	5.4	0.11	0.84	0.7	0.87	0.02	3.64	8

*Source: Authors (2023).*

It can be observed in Table 1, from the values shown, that there is low variability in the turbidity data sample, with a difference between the highest and lowest values of 4.36 NTU. Next, with the training and prediction by the Machine Learning algorithms, it was possible to obtain the discrepancy values between the observed and predicted turbidity presented by each method. Thus, an exploratory statistical analysis of the discrepancies was performed (Table 2).

*Table 2 – Exploratory Analysis of Turbidity Discrepancies for each Machine Learning Algorithm*

	RF (Random Forest)	ANN (Artificial Neural Network)	SVM (Support Vector Machine)	GBM (Gradient Boosting Machine)
<b>Mean (NTU)</b>	-0.002	-0.003	-0.007	-0.004
<b>Standard Error (NTU)</b>	0.001	0.002	0.002	0.002
<b>Median (NTU)</b>	0.000	0.006	-0.003	0.010
<b>Standard Deviation (NTU)</b>	0.143	0.254	0.241	0.238
<b>Sample Variance (NTU<sup>2</sup>)</b>	0.020	0.065	0.058	0.057
<b>Kurtosis</b>	19.195	2.823	5.594	4.133
<b>Skewness</b>	-0.527	-0.049	-0.595	-0.527

*Source: Authors (2023).*

From the values illustrated in Table 2, it can be seen that RF presented lower values for mean, standard error, median, standard deviation, and variance of the discrepancies, indicating better performance. Among the other algorithms, ANN had the lowest mean; however, its standard deviation, variance, and median were relatively higher than those of SVM and GBM. Ma et al. (2021) also tested Machine Learning algorithms, where RF and GBDT, similar to GBM, showed the best performance for RMSE and R<sup>2</sup> compared to SVM, KNN, and ELM (Extreme Learning Machine).

To complement the exploratory analyses, scatter plots for the predicted and observed values were created (Figure 5).

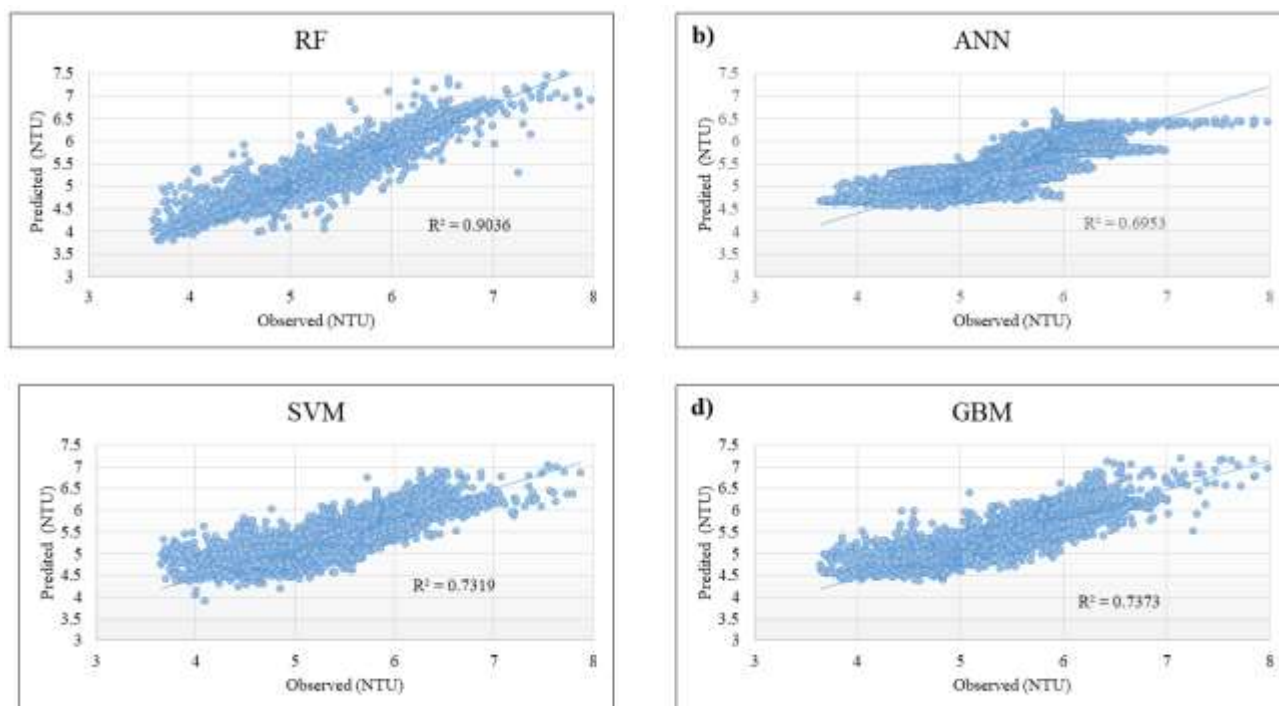


Figure 5 – Scatter plots between predicted and observed values. a) RF (Random Forest); b) ANN (Artificial Neural Networks); c) SVM (Support Vector Machine); d) GBM (Gradient Boosting Machine).

Source: Authors (2023).

It can be observed (Figure 5) that the RF and GBM algorithms show less sample dispersion, with higher R<sup>2</sup> values of 0.90 and 0.74, respectively. This indicates that RF showed less dispersed and more consistent values with those observed. ANN did not make accurate predictions for turbidity values below 4.5 NTU or above 6.5 NTU. SVM had greater difficulty predicting turbidity for values above 7.0 NTU.

Uncertainty calculation was performed using RMSE and MAE for performance analysis and R<sup>2</sup> for correlation evaluation of each algorithm (Table 3).

Table 3 – Performance evaluation for each Machine Learning algorithm according to RMSE (Root Mean Square Error),

	RMSE (NTU)	MAE (NTU)	R <sup>2</sup>
ANN	0.25	0.18	0.70
SVM	0.60	0.46	0.73
GBM	0.24	0.17	0.74
RF	0.14	0.07	0.90

MAE (Mean Absolute Error), and R<sup>2</sup> (Correlation Coefficient) parameters.

Source: Authors (2023).

It is noteworthy that in this uncertainty analysis (Table 3), RF showed the best performance, with RMSE values of 0.14 NTU and MAE of 0.07 NTU. It was followed by GBM with an RMSE of 0.24 NTU and an MAE of 0.17 NTU. Although ANN presented values close to GBM, the scatter plot analysis previously conducted indicates that ANN does not fit well as a model for the data in question. Ma *et al.* (2021) also found low performance using ANN and SVM for turbidity estimation with Sentinel 2A images in northeastern China. Li *et al.* (2023) achieved the best water turbidity prediction using the RF algorithm for Sentinel 3 images, with the best RMSE and  $R^2$  values.

Subsequently, Digital Turbidity Models were generated using the IDW interpolator for each Machine Learning method (Figure 6).

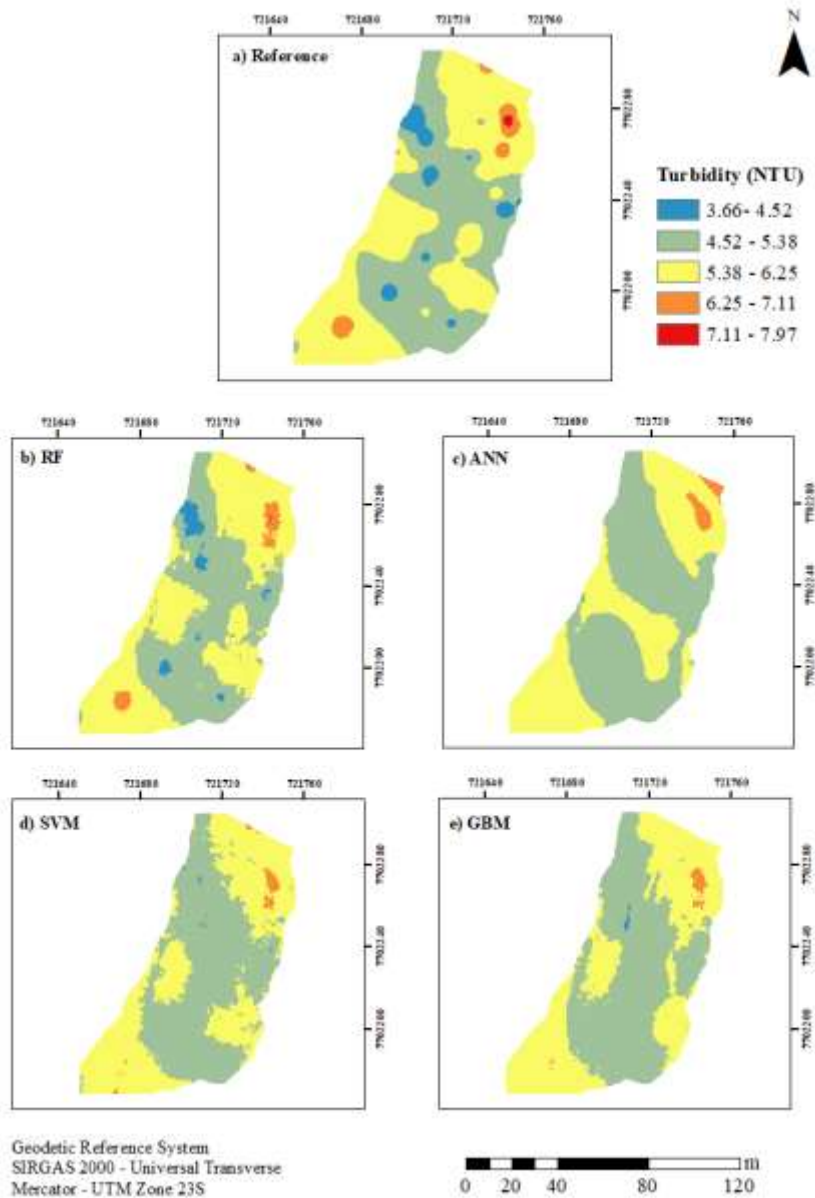


Figure 6 – DTMs for the Machine Learning methods a) Reference; b) RF (Random Forest); c) ANN (Artificial Neural Networks); d) SVM (Support Vector Machine); e) GBM (Gradient Boosting Machine).

Source: Authors (2023).

The DTMs significantly aid in the spatial visualization of the estimated turbidity for each algorithm. In this regard, analyzing Figure 6, it can be seen that RF is the method that most closely matches the reference DTM of the reservoir, presenting similar points with high and low turbidity values. On the other hand, the other algorithms show modeling with less similarity to the reference DTM, especially ANN, where turbidity values were smoothed. Authors like Keller et al. (2018) also observed poorer performance of models with ANN, using the Backpropagation algorithm on hyperspectral images.

It is believed that RF showed the best performance in all analyses due to its robustness and lower sensitivity to potential outliers that may exist in the data set. Additionally, RF is capable of constructing independent decision trees, making it more effective in noisy data. Generally, ANN is not very effective in samples contaminated with outliers and in cases of high data complexity; the network architecture must be modified numerous times to obtain the best result, potentially generating significant computational effort (Raudys & Jain, 1990; Yeo & Johnson, 2000; Bishop, 2006).

#### 4. Final Considerations

The continuous study and monitoring of rivers and reservoirs is crucial for the effective management of available water resources worldwide. Turbidity is an essential parameter for drawing conclusions about the quality of a water body. In this context, the results presented highlight the effectiveness of using RPA images associated with Machine Learning techniques to estimate water turbidity in reservoirs. This proposed approach can be applied on a large scale to monitor water quality in reservoirs, providing valuable information for organizations responsible for water resource management.

The use of Machine Learning techniques, particularly RF, can significantly aid in accurately, quickly, and cost-effectively predicting water turbidity in reservoirs. It can also be affirmed that GBM is a potential algorithm for use in this context; however, further tests in different study areas with varying hyperparameters should be conducted for such confirmation.

Therefore, it is recommended for future work to execute the study in different areas and to alternate the hyperparameters of ANN to avoid excessive computational effort. The SVM algorithm can also be improved by altering hyperparameters and changing the study area. Additionally, performing an outlier detection analysis in the original data set can provide even more optimized predictions for the Machine Learning algorithms.

#### Acknowledgements

This work was supported by CNPq – Conselho Nacional de Desenvolvimento Científico e Tecnológico.

#### References

- AGISOFT LLC. Agisoft Metashape 1.8.0—Professional edition: Agisoft LLC software.2023
- AKSO. Turbidímetro Digital TU340. Disponível em: <https://akso.com.br/product/turbidimetro-digital-tu430/>
- ALLAM, M.; YAWAR ALI KHAN, M.; MENG, Q. Retrieval of turbidity on a spatio-temporal scale using Landsat 8 SR: a case study of the Ramganga River in the Ganges Basin, India. **Applied Sciences**, v. 10, n. 11, p. 3702, 2020.DOI: <https://doi.org/10.3390/app10113702>
- ANDRADE, L. C.; FERREIRA, I. O.; SANTOS, F. C. M.; TEIXEIRA, V. G. Estimativa do grau de assoreamento de reservatórios de captação de água: estudo de caso: reservatório da hidráulica, Universidade Federal de Viçosa, Viçosa, Minas Gerais. *Revista Brasileira de Geomática*, 8(1), 040-055.2020.DOI: 10.3895/rbgeo.v8n1.10074
- AWANGE, K. Global freshwater resources. In *Food Insecurity & Hydroclimate in Greater Horn of Africa: Potential for Agriculture Amidst Extremes* (pp.67-83). Cham: Springer International Publishing.2022. DOI: <https://doi.org/10.1007/978-3-030-91002-0>
- BISHOP, C. M. *Pattern Recognition and Machine Learning*. Springer. Capítulo 5: Neural Networks. 2006. ISSN: 1613-9011.

- BONANSEA, M.; RODRIGUEZ, M. C.; PINOTTI, L.; FERRERO, S. Using multi-temporal Landsat imagery and linear mixed models for assessing water quality parameters in Rio Tercero reservoir (Argentina). *Remote Sensing of Environment*, v.158, p.28-41.2015. DOI: <https://doi.org/10.1016/j.rse.2014.10.032>
- CAHALANE, C.; MAGEE, A.; MONTEYS, X.; CASAL, G.; HANAFIN, J.; HARRIS, P. A comparison of Landsat 8, RapidEye and Pleiades products for improving empirical predictions of satellite-derived bathymetry. *Remote sensing of environment*, v. 233, p. 111414, 2019. DOI: <https://doi.org/10.1016/j.rse.2019.111414>
- CASAL, G.; MONTEYS, X.; HEDLEY, J.; HARRIS, P.; CAHALANE, C.; MCCARTHY, T. Assessment of empirical algorithms for bathymetry extraction using Sentinel-2 data. *International Journal of Remote Sensing*, 40(8), 2855-2879.2019. DOI: <https://doi.org/10.1080/01431161.2018.1533660>
- DEZORDI, R.; KRAMER, G.; DA ROSA, C. N.; DAL OSTO, J. & FILHO, W. P. Análise Da Turbidez Superficial A Partir De Imagens Do Landsat-8 (Sensor OLI) Em Compartimento Aquático Do Reservatório De Itaipu-Pr, Brasil. Anais do XIX Simpósio Brasileiro de Sensoriamento Remoto. 14 a 17 de Abril de 2019. INPE – Santos – SP, Brasil. ISBN: 978-85-17-00097-3.2019.
- ESRI. ArcGIS Desktop: Release 10.5 [Software de computador]. Esri. 2016. <https://www.esri.com/>
- FERREIRA, Í. O.; RODRIGUES, D. D.; SANTOS, G. R.; Coleta, processamento e análise de dados batimétricos: Representação computacional do relevo submerso utilizando interpoladores determinísticos e probabilísticos. 1 ed. Alemanha: Saarbrücken, 2015. 100p.
- FUNASA. Fundação Nacional de Saúde. Manual de Controle da Qualidade da Água para Técnicos que Trabalham com ETAS. 2015.
- GLEICK, P.H. Global freshwater resources: soft-path solutions for the 21st century. *Science*, 302(5650), 1524-1528. 2003. DOI: [10.1126/science.1089967](https://doi.org/10.1126/science.1089967)
- HARIMOORTHY, K.; THANGAVELU, M. Multi-disease prediction model using improved SVM-radial bias technique in healthcare monitoring system. *Journal of Ambient Intelligence and Humanized Computing*, v. 12, n. 3, p. 3715-3723, 2021. DOI: <https://doi.org/10.1007/s12652-019-01652-0>
- HONG, H.; PRADHAN, B.; JEBUR, M. N.; BUI, D. T.; XU, C. & AKGUN, A. Spatial prediction of landslide hazard at the Luxi area (China) using support vector machines. *Environmental Earth Sciences*, 75(1), 1-14.2016. DOI: <https://doi.org/10.1007/s12665-015-4866-9>
- HOSSAIN, A. A.; MATHIAS, C.; BLANTON, R. Remote sensing of turbidity in the Tennessee River using Landsat 8 satellite. *Remote Sensing*, v. 13, n. 18, p. 3785, 2021. DOI: <https://doi.org/10.3390/rs13183785>
- HYPACK. HYPACK® (Versão 2021) [Software de computador]. HYPACK - A Xylem Brand. 2021. <https://www.hypack.com/>
- KELLER, S.; MAIER, P. M.; RIESE, F. M.; NORRA, S.; HOLBACH, A.; BÖRSIG, N. & HINZ, S. Hyperspectral data and machine learning for estimating CDOM, chlorophyll a, diatoms, green algae and turbidity. *International journal of environmental research and public health*, 15(9), 1881. 2018. DOI: <https://doi.org/10.3390/ijerph15091881>
- LACAUX, J. P.; TOURRE, Y. M.; VIGNOLLES, C.; NDIONE, J. A.; LAFAYE, M. Classification of ponds from high-spatial resolution remote sensing: Application to Rift Valley Fever epidemics in Senegal. *Remote Sensing of Environment*, 106(1), 66-74.2007. DOI: <https://doi.org/10.1016/j.rse.2006.07.012>
- LI, Y.; LI, S.; SONG, K.; LIU, G.; WEN, Z.; FANG, C.; ZHANG, L. Sentinel-3 OLCI observations of Chinese lake turbidity using machine learning algorithms. *Journal of Hydrology*, 622, 129668.2023. DOI: <https://doi.org/10.1016/j.jhydrol.2023.129668>

- MA, Y.; SONG, K.; WEN, Z.; LIU, G.; SHANG, Y.; LYU, L.; HOU, J. Remote sensing of turbidity for lakes in northeast China using Sentinel-2 images with machine learning algorithms. *IEEE Journal of Selected Topics in Applied Earth Observations and Remote Sensing*, 14, 9132-9146.2021. DOI: 10.1109/JSTARS.2021.3109292
- MATEO-PÉREZ, V.; CORRAL-BOBADILLA, M.; ORTEGA-FERNÁNDEZ, F.; VERGARA-GONZÁLEZ, E. P. Port bathymetry mapping using support vector machine technique and sentinel-2 satellite imagery. *Remote sensing*, 12(13), 2069.2020. DOI: <https://doi.org/10.3390/rs12132069>
- O'REILLY, C. M.; ALIN, S. R.; PLISNIER, P. D.; COHEN, A. S.; MCKEE, B. A. Climate change decreases aquatic ecosystem productivity of Lake Tanganyika, Africa. *Nature*, 424(6950), 766-768. 2003.
- PRIOR, Elizabeth M.; O'DONNELL, F. C.; BRODBECK, C.; DONALD, W. N.; RUNION, G. B.; SHEPHERD, S. L. Measuring high levels of total suspended solids and turbidity using small unoccupied aerial systems (sUAS) multispectral imagery. *Drones*, v. 4, n. 3, p. 54, 2020. DOI: <https://doi.org/10.3390/drones4030054>
- R CORE TEAM. R: A language and environment for statistical computing (Version 4.3.1) [Software]. R Foundation for Statistical Computing.2023. <https://www.R-project.org/>
- RAUDYS, S. J.; JAIN, A. K. Small sample size effects in statistical pattern recognition: Recommendations for practitioners. *IEEE Transactions on Pattern Analysis and Machine Intelligence*, 13(3), 252-264.1990. DOI: 10.1109/ICPR.1990.118138
- SU, T.C.; CHOU, H.T. Application of multispectral sensors carried on unmanned aerial vehicle (UAV) to trophic state mapping of small reservoirs: A case study of Tain-Pu reservoir in Kinmen, Taiwan. *Remote Sensing*, v.7, n.8, p.10078-10097.2015. DOI: <https://doi.org/10.3390/rs70810078>
- TOPOMAP. GNSS RTK T10. Disponível em: <https://topomap.com.br/>
- VERRELST, J.; MUÑOZ, J.; ALONSO, L.; DELEGIDO, J.; RIVERA, J.P.; CAMPSVALLS, G.; MORENO, J. Machine learning regression algorithms for biophysical parameter retrieval: Opportunities for Sentinel-2 and -3. *Remote Sens. Environ.* 2012, 118, 127–139. DOI: <https://doi.org/10.1016/j.rse.2011.11.002>
- WOOLWAY, R. I.; KRAEMER, B. M.; LENTERS, J. D., MERCHANT, C. J., O'REILLY, C. M., & Sharma, S. Global lake responses to climate change. *Nature Reviews Earth & Environment*, 1.8:388-403.2020. DOI: <https://doi.org/10.1038/s43017-020-0067-5>
- XIAO, X.; I. A. O.; JIAN, X. U.; DENG-ZHONG, Z. H. A. O.; BAO-CHENG, Z. H. A. O.; JIAN, X. U.; XUE-JUN, C. H. E. N. G.; GUO-ZHONG, L. I. Research on Combined Remote Sensing Retrieval of Turbidity for River Based on Domestic Satellite data. *Journal of Changjiang River Sci. Res. Inst*, v. 38, p. 128, 2021. DOI: 10.11988/ckyyb.20200337
- YANG, W.; ZHAO, Y.; WANG, D.; WU, H.; LIN, A.; HE, L. Using Principal Components Analysis and IDW Interpolation to Determine Spatial and Temporal Changes of Surface Water Quality of Xin'anjiang River in Huangshan, China. *Int. J. Environ. Res. Public Health*, 17, 2942.2020. <https://doi.org/10.3390/ijerph17082942>
- YEO, I. K.; JOHNSON, R. A. A new family of power transformations to improve normality or symmetry. *Biometrika*, 87(4), 954-959.2000. DOI: <https://doi.org/10.1093/biomet/87.4.954>
- ZHAO, D.; CAI, Y.; JIANG, H.; XU, D.; ZHANG, W.; An, S. Estimation of water clarity in Taihu Lake and surrounding rivers using Landsat imagery. *Advances in Water Resources*, v.34, n.2, p. 165-173, 2011. DOI: <https://doi.org/10.1016/j.advwatres.2010.08.010>

